



OPEN

Single-shot measurement of $> 10^{10}$ pulse contrast for ultra-high peak-power lasersSUBJECT AREAS:
NONLINEAR OPTICS
HIGH-FIELD LASERS
ULTRAFAST LASERSYongzhi Wang¹, Jingui Ma¹, Jing Wang², Peng Yuan², Guoqiang Xie², Xulei Ge², Feng Liu², Xiaohui Yuan², Heyuan Zhu¹ & Liejia Qian¹¹Shanghai Engineering Research Center of Ultra-precision Optical Manufacturing, Department of Optical Science and Engineering, Fudan University, Shanghai 200433, China, ²Key Laboratory for Laser Plasmas (Ministry of Education), Department of Physics and Astronomy, Shanghai Jiao Tong University, Shanghai 200240, China.Received
9 October 2013Accepted
3 January 2014Published
22 January 2014Correspondence and
requests for materials
should be addressed to
L.J.Q. (ljqian@fudan.
edu.cn)

Real-time pulse-contrast observation with a high dynamic range is a prerequisite to tackle the contrast challenge in ultra-high peak-power lasers. However, the commonly used delay-scanning cross-correlator (DSCC) can only provide the time-consuming measurements for repetitive lasers. Single-shot cross-correlator (SSCC) becomes essential in optimizing laser systems and exploring contrast mechanisms. Here we report our progress in developing SSCC towards its practical use. By integrating both the techniques of scattering-noise reduction and sensitive parallel detection into SSCC, we demonstrate a high dynamic range of $> 10^{10}$, which, to our best knowledge, is the first demonstration of an SSCC with a dynamic range comparable to that of commercial DSCCs. The comparison of high-dynamic measurement performances between SSCC and a standard DSCC (Sequoia, Amplitude Technologies) is also carried out on a 200 TW Ti:sapphire laser, and the consistency of results verifies the veracity of our SSCC.

Pulse contrast, defined as the ratio of peak intensity of the main pulse to its background, is critical for well-controlled laser-matter interaction experiments such as the laser-based particle acceleration^{1–4}. Extremely high contrast of $\sim 10^{10}$ is required for femtosecond lasers with peak power of hundreds of terawatt to petawatt^{5–9}. Real-time contrast observation, relying on measuring the pulse profile within a large temporal window, is a prerequisite to solve the contrast problem^{10–14}, and is also one of the most challenging tasks in the field of measurement. While delay-scanning cross-correlator (DSCC) can resolve such high contrast¹⁵, it is appropriate only for repetitive laser systems, and typically takes tens of thousands of pulses and tens of minutes for one measurement. Therefore, this kind of time-consuming measurement was usually adopted to examine the contrast parameter for a laser system after construction, and could hardly be applied for exploring unknown contrast mechanisms and optimizing laser systems.

Recently, spectrogram techniques such as Wizzler¹⁶, FROG^{17,18} and SRSI¹⁹ were widely accepted in characterizing femtosecond pulses, and can be also operated in single-shot mode. This kind of measurement typically reveals temporal information within 1 ~ 25 ps over a dynamic range of $\sim 10^6$. To extend these methods to pulse contrast measurement, considerable difficulties in spectral resolution (i.e., temporal window) and intensity accuracy will be unavoidable. For example, an accuracy of 10^{-10} for pulse spectrum measurement is required for resolving a contrast of 10^{10} , which is significantly beyond the best capability of spectrogram-based instruments.

Single-shot cross-correlator (SSCC) is the most promising technology for real-time contrast observation. In a cross-correlation measurement in the form of either SSCC or DSCC, the pending test (PT) pulse is mixed with a clean sampling pulse in a nonlinear crystal, and the average power of the generated signal is recorded as a function of the relative delay between the two pulses. Different from scanning by mechanical motion in DSCC, the time delay in SSCC is realized normally by time-to-space encoding (see methods) in a non-collinear mixing configuration^{20,21}, so that the contrast can be measured with an isolated pulse. For practical contrast measurement, however, two major constraints still exist in SSCC. First, the typically reported dynamic range of SSCC is only about 10^6 – 10^7 , which is far from the stringent requirement of ultra-high peak-power lasers^{22–26}. Second, there is a lack of direct verification on the veracity of single-shot measurement.

While previous work devoted to the SSCC elementary technologies such as dynamic range and temporal window, here we focus on investigating the ultimate capability of SSCC instrument and comparing the high-dynamic measurement performances between SSCC and a standard DSCC. The single-shot measurement of pulse contrast as high as 10^{10} is reported for the first time. This ability opens the door for real-time contrast study



of laser systems in the power regime of hundreds of terawatt to petawatt. To demonstrate the practical use of SSCC, the pulse contrast of a commercial 200-TW Ti:sapphire laser system (Pulsar, Amplitude Technologies) is characterized in single-shot, which is consistent with the standard DSCC measurement.

The dynamic range of SSCC is mainly determined by the ability of sensitively and accurately detecting the lowest pulse side-lobe or background. Due to the time-to-space encoding in SSCC, the background of the measured pulse will be contaminated by optical scattering of the signal peak (i.e., the main pulse). This contamination can be dramatically reduced by placing a dot-mirror at the signal peak in space²⁴. On the other hand, a fiber-array-based detection system may perform parallel to serial mapping and allow the use of a sensitive photomultiplier tube (PMT)²¹. In this letter, we show that combination of these two techniques may lead an SSCC to support a dynamic range of $>10^{10}$, proved by testing the cleaned femtosecond pulse from cross-polarized wave generation (XPW)²⁷. The demonstrated dynamic range exceeds previously reported values for SSCC by several orders of magnitude.

To verify the veracity of the single-shot measurement, we compare the experimental results obtained by our SSCC and a standard DSCC (Sequoia 800, Amplitude Technologies) for three femtosecond Ti:sapphire laser systems with power from ~ 3 GW to 200 TW and pulse contrast from 10^6 to $>10^{10}$. This is the first measurement comparison between SSCC and DSCC. The good agreement in the comparison renders our SSCC a promising tool for the real-time contrast observation that may play a significant role in the field of ultra-high peak-power lasers.

Results

Experimental setup and design. The experimental setup employed in this work consists of three parts: femtosecond laser sources, an SSCC, and a commercial DSCC (Sequoia). Throughout our experiments, three kinds of femtosecond Ti:sapphire lasers at 800 nm (Fig. 1(a)) were adopted as the source of PT pulses successively. The first one, operating at a repetition rate of 1 kHz, is a commercial Ti:sapphire regenerative amplifiers (Legend Elite, Coherent) with a pulse energy of 3.5 mJ and duration of 35 fs. For the purpose of testing the limit of dynamic range, the output pulse from this laser was temporally cleaned by using the technique of XPW (see Methods), resulting in a pulse energy of ~ 100 μ J and a peak power of ~ 3 GW, which served as the second source of PT pulses. The third one, operating at 10 Hz, is a commercial Ti:sapphire laser system (Pulsar, Amplitude Technologies) with an ultra-high peak power of 200 TW and a duration of 25 fs. Since all the three femtosecond lasers are repetitive, their pulse contrasts can

also be measured by Sequoia (see Methods) for the performance comparison with the SSCC.

The design of SSCC is illustrated in Fig. 1(b). The sampling pulse (~ 100 μ J), at a wavelength of 1040 nm, was generated by a lithium-niobate-based optical parametric amplifier (OPA) system (see Methods for full details) pumped by the femtosecond pulse (~ 1 mJ) from the laser under test. In a femtosecond OPA, only the main peak of signal pulse experiences the OPA gain within the temporal window set by the pump duration. According to Ref. 28, the output pulse from an OPA can be cleaner than its pump pulse under the condition of sufficient OPA gain. Both beams of the sampling and PT pulses were cylindrically focused onto a type-I phase-matched 1.5-mm-thick β -BBO crystal to produce the correlating signal via sum-frequency generation (SFG). At the input face of the crystal, the two beams overlapped in an area of approximately 15 mm \times 150 μ m. The intersecting angle was $\sim 39^\circ$, which provided a temporal delay window of ~ 50 ps across the beams.

The SSCC adopts both the techniques of scattering-noise reduction and sensitive parallel detection for achieving a high dynamic range. In order to reduce the measurement contamination by air scattering of the signal peak, one or double dot-mirror(s) (see Methods) with an attenuation of $500\times$ for each was placed right after the crystal to greatly reduce the main peak of the SFG signal in space. In addition, the β -BBO crystal was designed with a wedged angle of 3° to avoid another kind of contamination from the surface reflections²⁴. The spatially distributed SFG signal was then imaged by a cylindrical lens onto a fiber array consisting of 100 fibers with different lengths (~ 1 m increment between successive fibers), and converted into a series of temporally separated pulses which were captured by a high-sensitivity PMT (H10721-210, Hamamatsu). In the case of measuring a high contrast of $\sim 10^{10}$, a set of attenuators (20 dB) was applied to the fiber-array detection system to accommodate to the dynamic range of PMT. Finally, the output of PMT was displayed on a 300-MHz oscilloscope.

Dynamic range and measurement veracity. The SSCC was first tested for the femtosecond Ti:sapphire regenerative amplifier. Figure 2 shows the measured pulse profile within a temporal window from -40 ps to 10 ps (black line with symbols). Since the pulse background is only about 10^{-6} relative to the peak of the main pulse, a dot-mirror with an attenuation of $500\times$ must be adopted to eliminate the measurement contamination. Pulse contrast of the Ti:sapphire regenerative amplifier was also measured by using a Sequoia (blue line), which can be regarded as a quite accurate reference for comparison. The two measurements show an excellent agreement, in terms of the pulse background, temporal

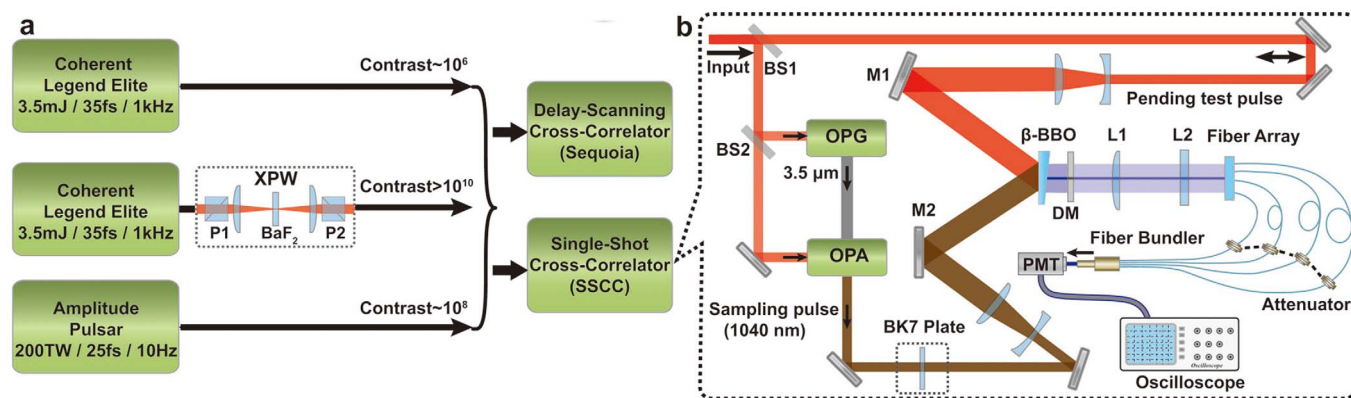


Figure 1 | (a) Experimental setup. Three femtosecond Ti:sapphire laser systems covering a power range of ~ 3 GW to 200 TW and a contrast range of 10^6 to $>10^{10}$ were adopted for the contrast measurements by using SSCC and Sequoia. (b) Diagram of SSCC. BS1 and BS2, beam splitters; M1 and M2, cylindrical concave mirrors with an equal focal length of 250 mm; DM, dot-mirror. L1 and L2, the imaging and coupling lenses with focal lengths of 200 mm and 30 mm, respectively.

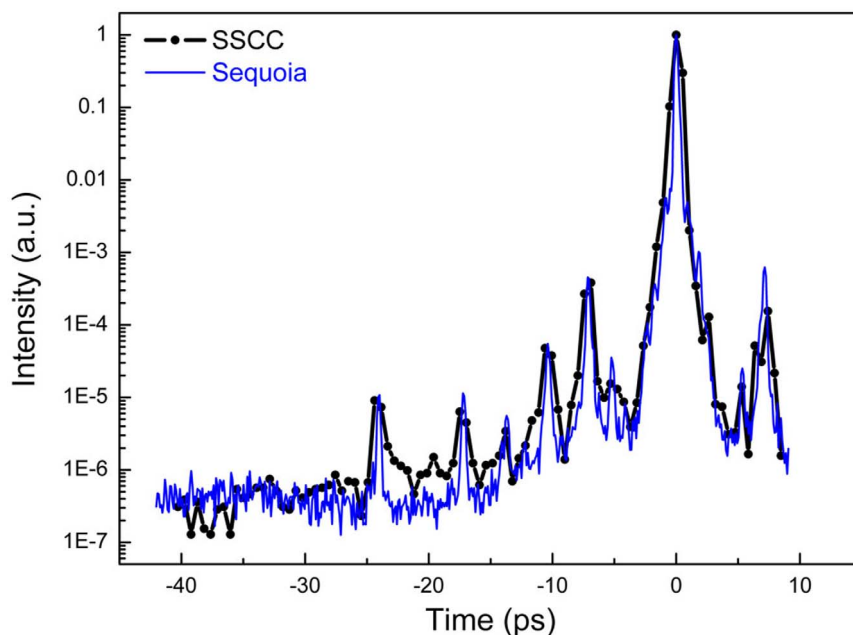


Figure 2 | The SSCC measurement (black line with symbols) versus Sequoia measurement (blue line) for the pulse profile of the femtosecond Ti:sapphire regenerative amplifier.

spikes, and the main pulse. The six tiny spikes appeared before the main pulse are real structures of the PT pulse rather than the measurement-introduced artifacts because of the comparison agreement. This proves the veracity of our single-shot measurement at a moderate contrast of $\sim 10^6$.

In order to determine the ultimate of the dynamic range supported by the SSCC, PT pulses with contrast higher than the device capability are required. We adopted XPW technique (see Methods) to clean the pulses from the femtosecond Ti:sapphire regenerative amplifier. Pulses with an estimated contrast of $\sim 10^{12}$ were obtained and served for this purpose. Figure 3(a) presents the measured pulse profiles after XPW cleaning by using the SSCC (black lines with symbols) and Sequoia (blue line). In the SSCC measurement, double dot-mirrors with an overall attenuation of 2.5×10^5 and a set of fiber attenuators (20 dB) were adopted to reduce the signal peak. The

background levels in the two measurements suggest that the dynamic ranges of SSCC and Sequoia are about 3×10^{10} and 5×10^9 , respectively. Tiny spikes at -27 ps and -32 ps, appearing in the SSCC measurement only, were identified as the artifacts caused by the beam splitters (BS1 and BS2 shown in Fig. 1). As shown in Fig. 3, the SSCC and Sequoia can resolve the pulse side-lobe or background as low as 3×10^{-11} and 2×10^{-10} , respectively. For pulse side-lobes or background stronger than 2×10^{-10} , there exhibits good consistence between the two measurements. Meanwhile, the pulse structures weaker than 2×10^{-10} , may be resolved by SSCC, but will be smeared out in the Sequoia measurement.

To further verify the veracity at such a high contrast of $\sim 10^{10}$, we applied SSCC to measuring some known weak temporal structures. For this purpose, a 1.1-mm-thick uncoated BK7 plate was inserted into the sampling beam to produce a series of pulse replicas with

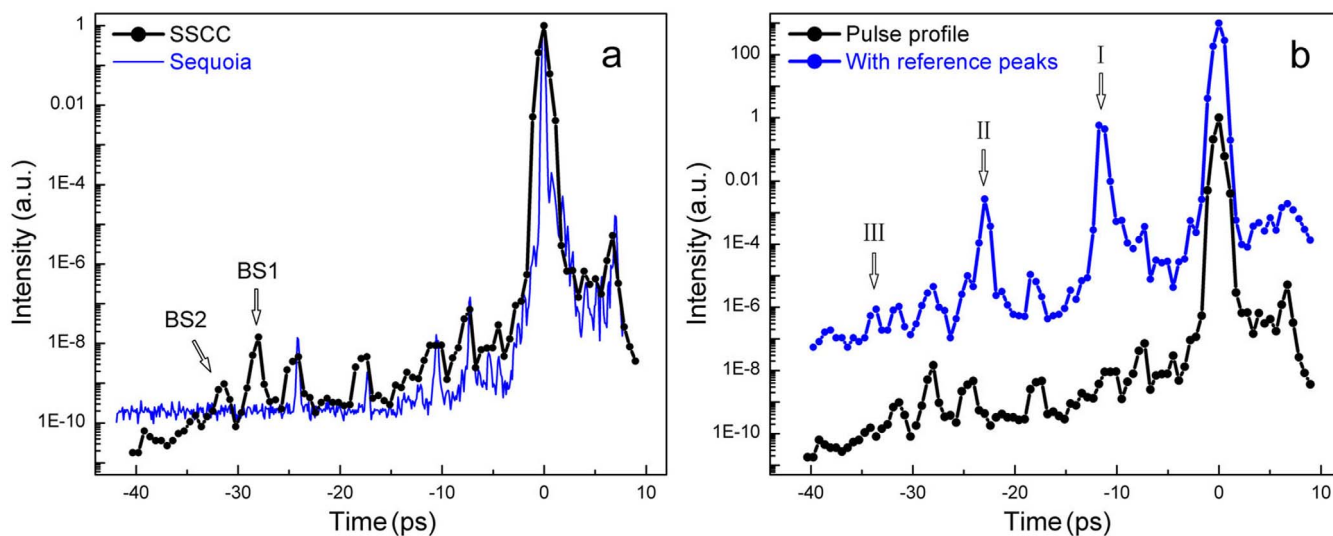


Figure 3 | (a) The SSCC measurement (black line with symbols) versus Sequoia measurement (blue line) for the pulse profile of the femtosecond pulses generated by XPW. Two artificial spikes caused by the beam splitters BS1 and BS2 are marked by arrows. (b) Two SSCC measurements for the femtosecond pulses generated by XPW with (blue line with symbols) and without (black line with symbols) a BK7 plate in the sampling arm. Three reference peaks caused by the multiple surface reflections in the BK7 plate are marked by arrows.

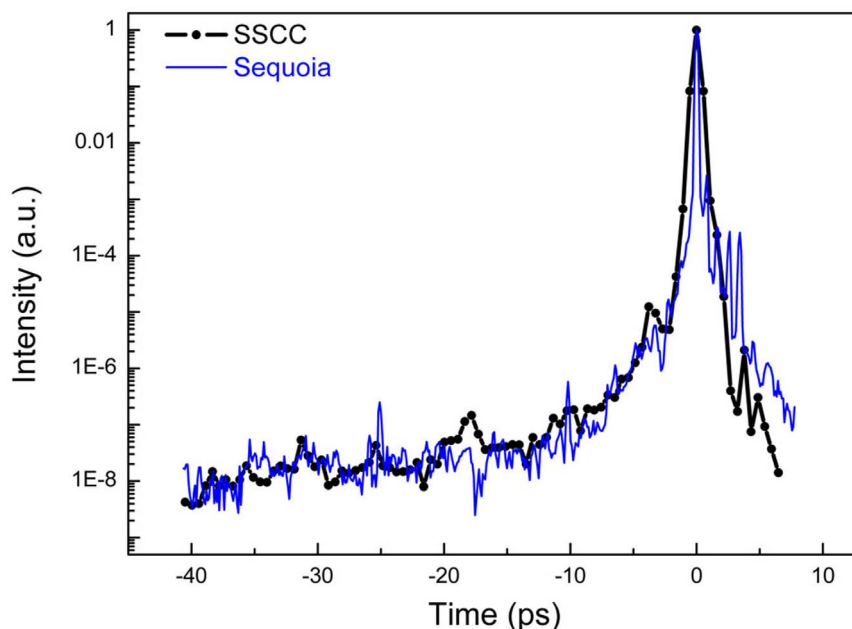


Figure 4 | The SSCC measurement (black line with symbols) versus Sequoia measurement (blue line) for the pulse profile of the 200 TW Ti:sapphire laser.

reduced intensities at the trailing edge of the sampling pulse due to surface reflections, which would be imprinted on the leading edge of the measured correlation trace. The measurement result for this situation is shown in Fig. 3(b). It is clear that the first (I), second (II) and third (III) pulse replicas appear at -11 ps, -22 ps and -33 ps, respectively. The measured intensities and locations of the three pulse replicas are consistent with the calculations based on Fresnel reflections. In particular, the evidence for capturing the third replica with a relative intensity as low as $\sim 10^{-9}$ clearly demonstrates the high capability in dynamic range of the SSCC.

Application to a 200-TW laser system. To demonstrate its performance in practical use, the SSCC was applied to characterizing the pulse contrast of a 200-TW femtosecond Ti:sapphire laser operating at a repetition rate of 10 Hz. While DSCC may still work at such a low repetition rate, it is time-consuming, e.g., it took about an hour to complete the measurement by Sequoia. The results obtained by SSCC (black line with symbols) and Sequoia (blue line) are presented in Fig. 4, which show a good agreement in both the background and main pulse. The measured pulse contrast of $\sim 2 \times 10^8$ is comparable to the reported values for similar systems²⁹.

Finally, the performance comparison of the SSCC versus other state-of-the-art pulse measurement techniques is summarized in Table 1, including conventional DSCC (e.g., Sequoia), Wizzler, FROG and SRSI. SSCC is definitely a promising tool for the real-time contrast observation.

Discussion

In conclusion, we have reported a high-dynamic-range SSCC and its application for an ultra-high peak-power laser. By resorting to a cleaned femtosecond pulse from XPW, and combining the techniques of scattering-noise reduction and sensitive fiber-array detection into an SSCC, we have demonstrated a dynamic range of $> 10^{10}$, which is several orders of magnitude improvement in single-shot mode. To the best of our knowledge, this is the first demonstration that an SSCC can support dynamic range as high as that of a commercial DSCC. At this point, it is important to address the scalability to higher dynamic-range. The correlating process in our SSCC is considered again, where the beam size at the correlating crystal was ~ 15 mm in the plane of intersection (space-to-time encoding) and ~ 150 μm in the lateral plane, respectively. The generated signal peak will be proportional to the lateral beam size under the condition of fixed intensities (i.e., sufficient pulse energy). Consequently, the dynamic range can be linearly scaled up since the contamination on pulse background can be effectively eliminated. Higher dynamic-range, e.g., $\sim 10^{12}$, is possible by the present route if the lateral beam size is increased from 150 μm to 15 mm. Such a device will be promising in constructing and optimizing ultra-high peak-power laser systems with power beyond petawatt.

Methods

DSCC. We adopted a commercial DSCC (Sequoia, Amplitude Technologies) to perform referential measurements of pulse contrast. The parameters of Sequoia are listed in Table 1.

Table 1 | Performances of the SSCC versus other techniques

Specifications	SSCC	Sequoia 800 (Amplitude Technologies)	FROG (Swamp Optics 8-1-pico GRENOUILLE)	Wizzler 800 (Fastlite)	FOX-SRSI ¹⁹
Dynamic range	$> 10^{10}$	$> 10^9$ (typical 10^{10})	$> 10^3$	$< 10^5$	$\sim 10^6$
Temporal window	~ 50 ps	570 ps	35 ps	< 5 ps	~ 25 ps
Resolution	~ 0.7 ps ⁽¹⁾	~ 250 fs ⁽²⁾ (17 fs/step)	~ 350 fs ⁽³⁾ (30 fs/pixel)	~ 20 fs ⁽⁴⁾	Unspecified
Operating mode	Single-shot	Delay-scanning	Single-shot & delay-scanning	Single-shot	Single-shot

⁽¹⁾Determined by measuring a much shorter pulse duration (~ 35 fs) of the femtosecond Ti:sapphire regenerative amplifier.

⁽²⁾Limited by its non-collinear correlating angle. It was determined in our experiment by measuring the pulse duration (~ 35 fs) of the femtosecond Ti:sapphire regenerative amplifier.

⁽³⁾ ⁽⁴⁾ Estimated from their maximum spectral ranges.



Time-to-space encoding. Crossing beams at a large angle produces a range of delay across the nonlinear crystal and maps time delay onto transverse position. In such a time-to-space encoding, the temporal window of SSCC is determined by the non-collinear angle as well as the beam width.

XPW. The XPW, illustrated in Fig. 1(a), consists of two Glan polarizers (GL10-B, Thorlabs), two convex lenses (focal length of 1 m) and a BaF₂ crystal (thickness of 2 mm). In the experiment, the partially-reflected portion of the main beam, with a pulse energy of 2 mJ, was loosely focused onto the BaF₂ crystal. With the proper settings of the elements involved, the high-intensity central portion of the pulse may pass through the second polarizer with a transmission of ~99%, while the low-intensity background is attenuated considerably with a residual transmission of ~10⁻⁶. The pulse energy after XPW was ~100 μJ, corresponding to an overall efficiency of ~5%. In principle, the improvement of pulse contrast by XPW follows cubic law in the ideal case. However, practically an improvement of ~10⁶ is typical due to limited extinction ratio of the polarizers.

OPA system. The femtosecond OPA system, illustrated in Fig. 1(b), consists of a stage of optical parametric generator (OPG) in a double-pass configuration, and an OPA stage. The pump beam, with pulse energy of 1 mJ, is a partially-reflected portion of the beam of PT pulses. Two 8-mm-thick uncoated MgO:LiNbO₃ crystals (supplied by CASTECH) both cut at $\theta = 46.5^\circ$ for type-I phase matching were used in the OPG and OPA stages, respectively. The pump beam was divided by a beam splitter (BS2) with a reflectance of ~20%, and the two beams were telescoped down to obtain the pump intensities of ~70 GW/cm² and ~50 GW/cm² for the two stages, respectively. To get a cleaner sampling pulse at 1040 nm, the output idler pulse of OPG at 3.5 μm was chosen to seed the OPA. The output pulse energy at 1040 nm was about 100 μJ, corresponding to an overall efficiency ~10%. The wavelength (i.e., 1040 nm) of sampling pulse was selected to support a larger noncollinear angle and accommodate to the peak response of the PMT as well.

Dot-mirror. The mirror has a diameter of 25 mm, and the central part (Φ1–2 mm) is coated for high reflection (99.8%) at the SFG wavelength (452 nm), while the rest part is uncoated.

Fiber-array detection system. The fiber-array detection system is based on a fiber-array and PMT. The fiber array consists of 100 fibers with incremental lengths from 3 m to 102 m. Each channel of the fiber array was spliced with calibrated fiber attenuators or a fiber connector. The fibers were aligned into a one-dimensional array on the input end, which was fabricated by high precision V-groove-based technique (Broadex Tech., China). The distal ends of the fibers were bound together and optically relayed onto a PMT. This technique performs the parallel to serial mapping and allows the use of a high sensitive single-point detector (i.e., PMT).

Operation of SSCC. The OPA-generated sampling pulse (1040 nm) and the pulse under test (800 nm) were shined onto a correlating crystal (β-BBO) and crossed with a non-collinear angle (39°). The intensity of generated SFG signal (452 nm) was maximized by tuning the crystal. The transverse distributed SFG signal was one-dimensionally imaged and coupled into the fiber array, and then detected by the PMT after a band-pass filter (452 nm). The strongest part of SFG signal was first reduced by dot-mirrors with certain attenuations (2.5 × 10⁵ in this work) placed right behind the crystal and further reduced by fiber attenuators (attenuations from 10 ~ 10³) spliced in those channels with strong signals. In such a way, the signal intensity in each channel can be managed to match with the detectable range of an 8-bit oscilloscope. Finally, the pulse profile of under test was retrieved by multiplying the signal intensity of each channel with its corresponding attenuation (i.e., the fiber attenuators and dot-mirrors).

1. Faure, J. *et al.* A laser–plasma accelerator producing monoenergetic electron beams. *Nature*. **431**, 541–544 (2004).
2. Mangles, S. P. D. *et al.* Monoenergetic beams of relativistic electrons from intense laser–plasma interactions. *Nature*. **431**, 535–538 (2004).
3. Salamin, Y. I. *et al.* Relativistic high-power laser–matter interactions. *Phys. Reports*. **427**, 41–155 (2006).
4. Leemans, W. P. *et al.* GeV electron beams from a centimetre-scale accelerator. *Nature Phys.* **2**, 696–699 (2006).
5. Mourou, G. A., Tajima, T. & Bulanov, S. V. Optics in the relativistic regime. *Rev. of Modern Phys.* **78**, 309 (2006).
6. Mikhailova, J. M. *et al.* Ultra-high-contrast few-cycle pulses for multipetawatt-class laser technology. *Opt. Lett.* **36**, 3145–3147 (2011).
7. Yu, T. J. *et al.* Generation of high-contrast, 30 fs, 1.5 PW laser pulses from chirped-pulse amplification Ti: sapphire laser. *Opt. Express*. **20**, 10807–10815 (2012).
8. Wang, Z. *et al.* High-contrast 1.16 PW Ti: sapphire laser system combined with a doubled chirped-pulse amplification scheme and a femtosecond optical-parametric amplifier. *Opt. Lett.* **36**, 3194–3196 (2011).
9. Kaluza, M. *et al.* Influence of the laser prepulse on proton acceleration in thin-foil experiments. *Phys. Rev. Lett.* **93**, 045003 (2004).

10. Tavella, F., Marcinkevicius, A. & Krausz, F. Investigation of the superfluorescence and signal amplification in an ultrabroadband multiterawatt optical parametric chirped pulse amplifier system. *New Journal of Physics*. **8**, 219 (2006).
11. Schimpf, D. N., Seise, E., Limpert, J. & Tünnemann, A. The impact of spectral modulations on the contrast of pulses of nonlinear chirped-pulse amplification systems. *Opt. Express*. **16**, 10664–10674 (2008).
12. Hooker, C. *et al.* Improving coherent contrast of petawatt laser pulses. *Opt. Express*, **19**, 2193–2203 (2011).
13. Didenko, N. V., Konyashchenko, A. V., Lutsenko, A. P. & Tenyakov, S. Y. Contrast degradation in a chirped-pulse amplifier due to generation of prepulses by postpulses. *Opt. Express*. **16**, 3178–3190 (2008).
14. Forget, N. *et al.* Pump-noise transfer in optical parametric chirped-pulse amplification. *Opt. Lett.* **30**, 2921–2923 (2005).
15. Divall, E. J. & Ross, I. N. High dynamic range contrast measurements by use of an optical parametric amplifier correlator. *Opt. Lett.* **29**, 2273–2275 (2004).
16. Ultrafast pulse measurement device <http://www.fastlite.com/en/cat465017-460522-Wizzler.html> (Accessed 22nd Sept 2013).
17. Frequency-resolved optical gating (FROG), http://www.swampoptics.com/products_grenoview.htm (Accessed 22nd Sept 2013).
18. Kaganovich, D. *et al.* Origin and control of the subpicosecond pedestal in femtosecond laser systems. *Opt. Lett.* **38**, 3635–3638 (2013).
19. Palaniyappan, S. *et al.* Single-Shot 60 dB Dynamic Range Laser Contrast Measurement Using Fourth-Order Cross-Correlation from Self-Referencing-Spectral-Interferometry (FOX-SRSI). *CLEO: Science and Innovations. Optical Society of America*. DOI: 10.1364/CLEO_SI.2013.AF1J.3 (2013).
20. Collier, J., Hernandez-Gomez, C., Allott, R., Danson, C. & Hall, A. A single-shot third-order autocorrelator for pulse contrast and pulse shape measurements. *Laser and particle beams*. **19**, 231–235 (2001).
21. Zhang, D. *et al.* Fiber-array-based detection scheme for single-shot pulse contrast characterization. *Opt. Lett.* **33**, 1969–1971 (2008).
22. Shah, R. C., Johnson, R. P., Shimada, T. & Hegelich, B. M. Large temporal window contrast measurement using optical parametric amplification and low-sensitivity detectors. *The European Physical Journal D*. **55**, 305–309 (2009).
23. Dorrer, C., Bromage, J. & Zuegel, J. D. High-dynamic-range single-shot cross-correlator based on an optical pulse replicator. *Optics Express*. **16**, 13534–13544 (2008).
24. Wang, Y., Yuan, P., Ma, J. & Qian, L. Scattering noise and measurement artifacts in a single-shot cross-correlator and their suppression. *Appl. Phys. B*. **101**, 501–508 (2013).
25. Montant, S., Villate, D. & Rouyer, C. Single shot temporal contrast measurement of subpicosecond pulses. *In Journal of Physics: Conference Series*. **244**, 032011 (2010).
26. Jovanovic, I. *et al.* High-dynamic-range, 200-ps window, single-shot cross-correlator for ultrahigh intensity laser characterization. *Power (au)*. **104**, 103 (2007).
27. Jullien, A. *et al.* Highly efficient temporal cleaner for femtosecond pulses based on cross-polarized wave generation in a dual crystal scheme. *Appl. Phys B*, **84**, 409–414 (2006).
28. Ma, J. *et al.* Single-shot cross-correlator using a long-wavelength sampling pulse. *Opt. Lett.* **36**, 978–980 (2011).
29. Fourmaux, S. *et al.* Laser beam wavefront correction for ultra high intensities with the 200 TW laser system at the Advanced Laser Light Source. *Opt. Express*. **16**, 11987–11994 (2008).

Acknowledgments

The work was partially supported by grants from the National Basic Research Program of China (973 Program) (2013CBA01505) and the Natural Science Foundation of China (61008017 and 11121504).

Author contributions

L.Q. and H.Z. conceived the original ideas. Y.W., J.M. and J.W. designed and implemented the experiments. X.G., F.L. and X.Y. operated the Sequoia and the laser sources. L.Q., P.Y. and G.X. supervised the experiments and took part in the data analysis. All the authors contributed to the preparation of the manuscript.

Additional information

Competing financial interests: The authors declare no competing financial interests.

How to cite this article: Wang, Y.Z. *et al.* Single-shot measurement of >10¹⁰ pulse contrast for ultra-high peak-power lasers. *Sci. Rep.* **4**, 3818; DOI:10.1038/srep03818 (2014).



This work is licensed under a Creative Commons Attribution-NonCommercial-ShareAlike 3.0 Unported license. To view a copy of this license, visit <http://creativecommons.org/licenses/by-nc-sa/3.0>